A Singly Curved Conformal Phased Array with Integrated Particles-Based CRLH Phase Shifters

Muhammad Ayaz and Irfan Ullah

***Abstract*—In this paper, a four unit cell micron-sized magnetic particles embedded composite right/left-handed (CRLH) transmission line metamaterial phase shifter is proposed. The variable phases are achieved by activating the micron-sized magnetic particles along the length of stub transmission lines of the CRLH transmission line structure. This causes to effectively change the inductance of stub transmission lines, which changes the phase of the RF signal. These structures can be activated in a symmetric or asymmetrical manner to obtain wide range of phase shifts. A prototype of cascaded four unit cell CRLH transmission line phase shifter with embedded silver-coated ferrites (magnetic particles) is designed, fabricated and tested for phase shifters applications. The measured phase response of the proposed phase shifter is in close agreement with the simulated phase response. Next, for the performance analysis of proposed phase shifter, a 1 × 4 conformal curved-shaped phased array operating at 5.8 GHz is fed with the four unit cell cascaded phase shifter in CST full-wave simulator. The conformal phased array with proposed integrated phase shifters was simulated for broadside pattern correction and main beam scanning at 20 degree on curved-shaped surface with different bend angles. The radiation pattern results obtained with the proposed integrated phase shifters are in close agreement with those obtained with direct excitation of the array.**

***Index Terms*—CRLH transmission line, conformal antenna, silver-coated magnetic particles, metamaterial transmission line, conformal array.**

Original Research Paper
DOI: 10.53314/ELS2327043A

I. Introduction

THE conformal antennas are gaining popularity in a variety of applications, including radar and mobile communication systems. The conformal phased arrays have shown promising solutions for curved platforms, because of their wide azimuthal coverage, compact volume, resistance to wind pressure, efficient array aperture, and smooth integration with the aero platforms [1]. Conformal phased array antennas are needed in military radars, on-board satellite communication payloads, aircraft wings and for installation on non-planar geometries of ships and trains. In literature, most of the conformal phased arrays are driven with commercially available phase shifters [2]–[7]. However, one of the major drawback of these commercially available phase shifters is the intentional/unintentional breakage of chip ICs (integrated circuits) and/or their inability of flexing on conformal shaped surfaces [8,9]. Recently a new phase shifter based on graphene material is designed, and its performance for integration with conformal antenna array is evaluated [10]. The required phase shift is achieved by changing the applied voltage and resistance of the graphene material. The graphene based phase shifter requires an external DC (direct current) power supply, which will increase the complexity for large antenna arrays.

Traditionally, switching elements (RF diodes) and tunable capacitance characteristic of varactor diodes are exploited in the composite right/left-handed (CRLH) transmission lines to achieve the variable phase responses [11]-[13]. External RF (radio frequency) chokes/capacitors are required to operate the microwave diodes to achieve different phase shifts. These external DC voltages degrade the efficiency of the phase compensation circuits [14]. The conventional phase shifters used in the conformal phased arrays cannot be integrated with antenna elements to make them flexible on conformal surfaces.

In the proposed work, a curved-shaped 1×4 conformal phased array is integrated with novel fully printable and conformal phase shifters based on CRLH transmission line. Micron-sized magnetically aligned particles [15] are embedded inside the CRLH structure to control its left-handed inductance and capacitance parameters. The variable phase shift is obtained by activating and deactivating the magnetic particles inside the CRLH transmission line: this varies the effective length of current flow in stub/fingers of the CRLH transmission line, which causes to change the inductance/capacitance parameters of the CRLH structure, thereby changing the phase response.

The proposed work is different from the similar work in [16]- [17] as follows: In [16], a cylindrical phased array driven by particles reinforced metamaterial phase shifters is proposed. The maximum phase shift of 45^o is achieved, while in this work, a maximum phase shift of 180^o is obtained by cascading four unit cell particles based CRLH phase shifter. In [16], the antenna elements in the array are separately excited with the phase shifters, while in this work, the conformal array is integrated with the proposed phase shifters on a single printed circuit board, paving the way for its integration on a fully conformal RF electronics applications. The work in [17] has explored the extended phase shift range up to 180^o using the particles reinforced CRLH structure. However, the beam scanning capability

Manuscript received on May 17th, 2022. Received in revised form on July 4th, 2023 and July 27th 2023. Accepted for publication on August 24th, 2023.

Muhammad Ayaz is a PhD student in the Department of Electrical & Computer Engineering, COMSATS University Islamabad, Abbottabad Campus, Pakistan (email: muhammadayaz@uetpeshawar.edu.pk).

by using only the linear patch antenna array is demonstrated. Each antenna element in the array is excited with different number of phase shifters to achieve the main beam scanning, which complicates the design. In the proposed work, all the antenna elements in the conformal array are excited with equal number of phase shifters, thus enabling the design much simpler as compared to [17]. In addition, the performance of proposed phase shifter is demonstrated using the array on a non-planar shaped surface, thus enabling the potential uses of proposed phase shifter on a more general array's geometry.

The conformal curved-shaped phased array driven with micron-sized magnetic particles embedded CRLH transmission line phase shifters has a wide range of applications, including radar, satellite communication, and possible integration with non-planar microwave electronics devices, where the existing chip based phase shifters have definite drawbacks.

The paper is organized as follows: the design and simulation results analysis of the proposed phase shifter is explained in Section II, followed by the measurement setup and results for the proposed phase shifter in Section III. Section IV evaluates the 1 × 4 singly curved conformal phased array with proposed integrated phase shifters in CST platform. Section V finally concludes the paper.

II. Design of Particles Embedded CRLH Phase Shifter

A. Single Unit Cell Phase Shifter

Initially, the micron-sized magnetically aligned particles [15] are embedded along the symmetrical length of stub lines in the metamaterial composite right/left-handed (CRLH) unit cell structure. The resulting new **CRLH** unit cell structure with embedded magnetic **P**articles is denoted as 'P-CRLH' phase shifter. The embedding procedure of particles is achieved using a structure called MRS (Magneto-static Responsive Structure) which is illustrated in Fig. 1. The MRS is made up of a small section of substrate with a cavity hole drilled in it and with top and bottom copper layers. Then, the micron-sized magneto-static particles are partially inserted in the cavity. In the absence of applied magnetic field, the magnetic particles inside the cavity settles down and the MRS acts as an off switch (MRS is deactivated). After application of a static magnetic field (with a tiny

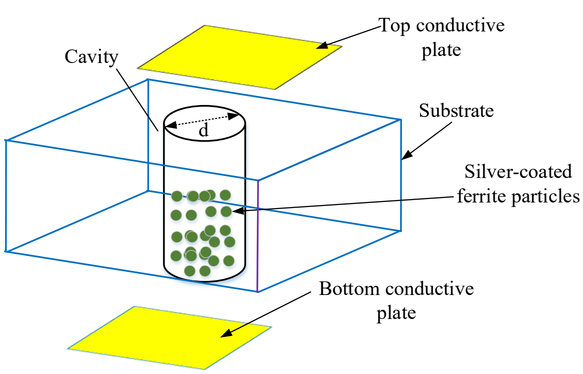

Fig. 1. MRS structure with silver-coated ferrite magnetic particles.

magnet) beneath the substrate section, the particles get aligned vertically in the direction of the applied magnetic field, connecting the two conductive copper layers (MRS is activated). The detailed procedure for designing and fabrication of MRSs are mentioned in [16]. Next, these MRSs are embedded along the length of stub lines of a CRLH structure as shown in Fig. 2 and are numbered as 1 to 16.

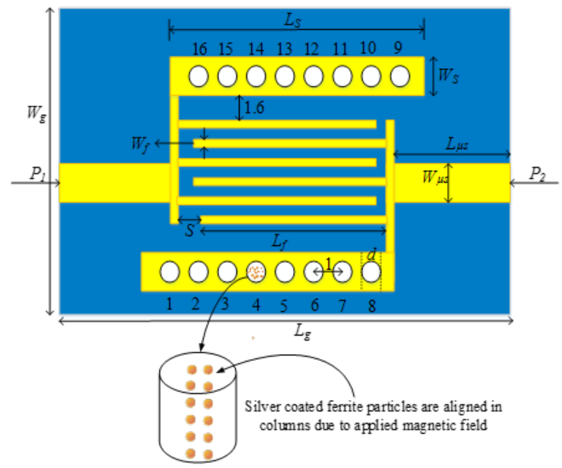

Fig. 2. A unit cell P-CRLH phase shifter. MRSs (numbered 1 to 16) are embedded in a unit cell CRLH transmission line acting as a variable phase shifter.

By activating and deactivating any MRS or group of MRSs, changes the physical length of stubs, which in turn changes the four structural parameters (L_L, C_L, L_R, C_R), and the phase behavior (ϕ_{21}) from port 1 to port 2 of the CRLH transmission line in Fig. 2 using the following expression [17]:

$$\phi_{21} = (\omega\sqrt{L_R C_R} - \frac{1}{\omega\sqrt{L_L C_L}} \times L_g \qquad (1)$$

where L_L, C_L are the left-handed inductance/capacitance, L_L, C_L are the right-handed inductance/capacitance and L_g is the physical length of the proposed phase shifter in Fig. 2. Equation (1) shows that the desired phase shift can be obtained by selecting the appropriate structural parameters (L_L, C_L, L_R, C_R) through designing the physical dimensions of phase shifter in Fig. 2.

B. Equivalent Circuit Modeling

The equivalent electronics circuit π-model of the unit cell P-CRLH phase shifter is developed using the approach in [19] and is shown in Fig. 3. The model consists of three sections labelled as microstrip transmission line (Microstrip TL), Stub Inductor (SI) and Inter-Digital Capacitor (IDC). The effects due to the physical length of microstrip TL in Fig. 2 is represented as series inductance $L_{\mu s}$ and the capacitance between microstrip TL and ground plane is represented as $C_{\mu s}$ in Fig. 3. The Stub Inductor (SI) section consists of series inductance L_s^{SI} (due to physical length of stub inductor), parallel inductance L_p^{SI} (due to magnetic particles in the cavity), and parallel capacitance C_p^{SI} (due to cavity). The IDC section consists of series induc-

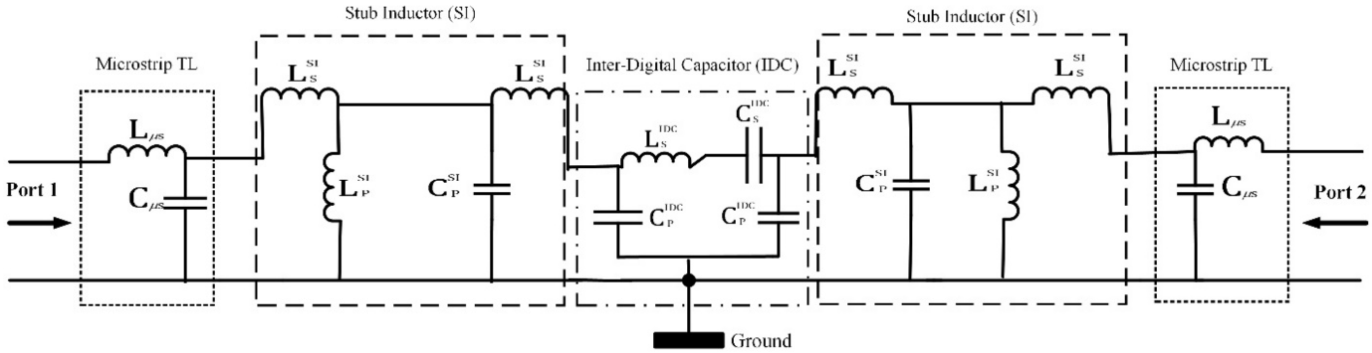

Fig. 3. Equivalent electronics circuit π-model of the proposed unit cell P-CRLH phase shifter. $L_{\mu s}$ = 0.5 nH, $C_{\mu s}$ = 0.36 pF, L_S^{SI} = 0.82 nH, L_P^{SI} = 1.47 nH, C_{PS}^{SI} = 0.36 pF, L_S^{IDC} = 0.64 nH, C_P^{IDC} = 1.72 pF, C_S^{IDC} = 2.85 pF.

tance L_s^{IDC} (due to physical length of fingers), series capacitance C_S^{IDC} (due to gaps among fingers), and parallel capacitance C_P^{IDC} (between fingers and ground plane). The numerical values of these model parameters are extracted using the procedure outlined in [17], and are given in the caption of Fig. 3. The four structural parameters in equation (1) are computed using the following expressions [18].

$$\left.\begin{aligned} L_R &= L_S^{IDC} + \frac{L_S^{SI}}{2} \\ L_R &= 2C_P^{IDC} + C_P^{SI} \\ L_L &= L_P^{SI} \\ C_L &= C_S^{IDC} \end{aligned}\right\} \quad (2)$$

The simulated MATLAB (using equation (1)), CST full-wave (using Fig. 2), and ADS circuit simulator (using circuit in Fig. 3) results for reflection coefficient, insertion loss and phase response are shown in Figs. 4 and 5. The CST results of S_{11} in Fig. 4 are below -10 dB over the desired frequency band (5-6 GHz), indicating good impedance matching characteristics. While S_{11} results in analytical/ADS schematic are -8 dB from 5 to 5.5 GHz and are below -10 dB onward 5.5 GHz. The mismatch between CST and analytical/circuit simulator results are due to the lossless analytical model assumption in Fig. 3. That is resistive/conductive losses are ignored in the circuit modeling.

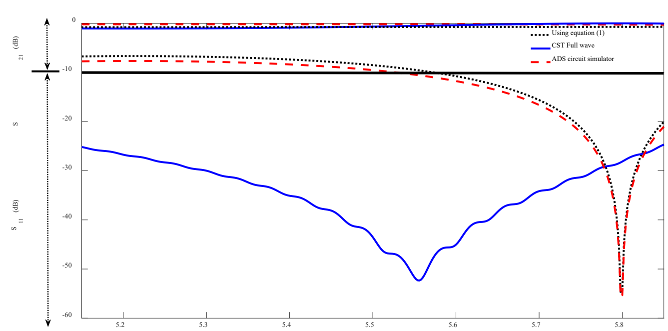

Fig. 4. Simulated analytical, circuit and full-wave results of reflection coefficient and insertion loss for the unit cell P-CRLH phase shifter (MRSs 1-3 and MRSs 9-11 are activated in Fig. 2).

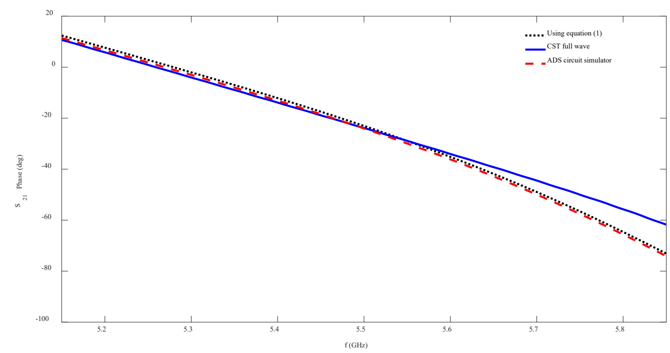

Fig. 5. Simulated analytical, circuit and full-wave results of phase response for the unit cell P-CRLH phase shifter (MRSs 1-3 and MRSs 9-11 are activated in Fig. 2).

The phase response in Fig. 5 is linear over the frequency band with slight deviations between CST and analytical/circuit simulator results due to perfect circuit modeling assumption.

C. Cascaded Unit Cells Phase Shifter

In this work, to obtain wider range of phase shifts, four unit cell are cascaded as shown in Fig. 6. The parametric study of MRSs activation on the S-parameters for a four unit cell P-CRLH phase shifter is given in Fig. 7. The CST simulated results of reflection coefficients and insertion losses are shown in Fig. 7(a). The reflection coefficient is less than 10 dB and maximum insertion loss is -2.2 dB over the operating C-band (5-6) GHz. The value of reflection coefficient is approximately -8 dB from 5-5.3 GHz and is below -10 dB beyond 5.3 GHz for MRSs 1-8 & 9-16 activation. This is due to taking out almost entire stub lines from the P-CRLH structure. Therefore, in this case, the only dominant parameter is inductive capacitance C_L in equations (1) and (2). The corresponding phase responses are shown in Fig. 7(b). The maximum step size (that is difference between phase slopes of MRSs 1 & 9 activation and MRSs 1-8 & 9-16 activation) of phase response varies from 180° to 250° over the 5-6 GHz band. The phase slope is almost constant and therefore the main beam scanning can be achieved with the proposed cascaded phase shifter.

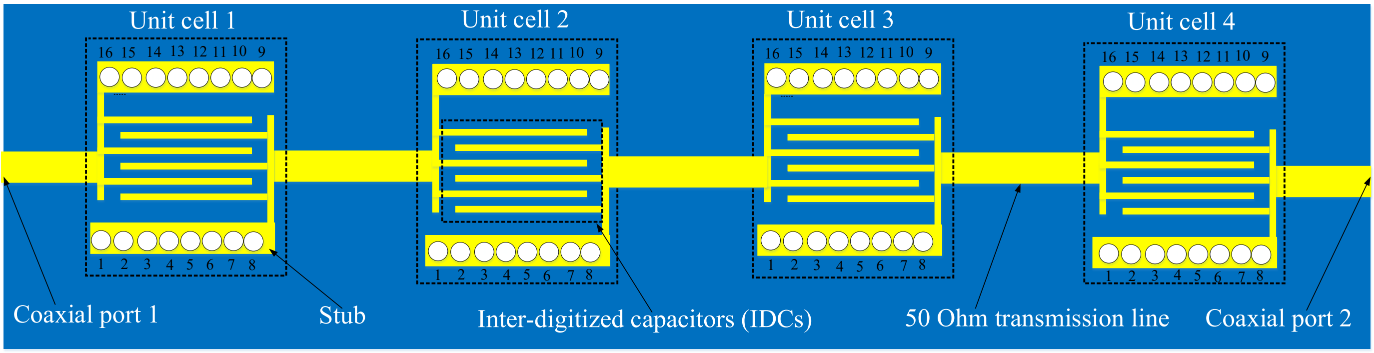

Fig. 6. Cascaded four unit cells P-CRLH phase shifter.

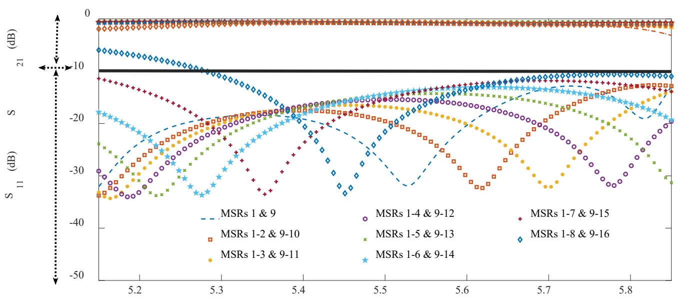

(a)

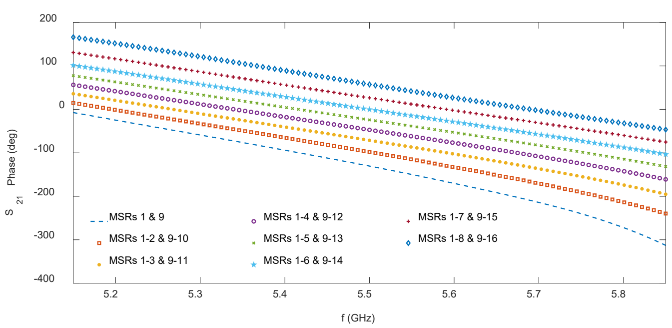

(b)

Fig. 7. CST simulated parametric study of cascaded four unit cell P-CRLH phase shifter for various MRSs activation. (a) reflection coefficients $|S_{11}|$ and insertion losses $|S_{21}|$ (b) phases $\angle S_{21}$.

III. Measurement Setup and Results

The measurement setup of the four unit cell fabricated P-CRLH phase shifter is shown in Fig. 8. The fabrication procedure is illustrated in [16, 17] and is not mentioned here. The cascaded P-CRLH phase shifter is connected to ports 1 and 4 of the in-house calibrated Agilent network analyzer (model no. E5071C). The small axial magnets beneath the MRSs are also shown in Fig. 8. The alignment (activation) of magnetic particles within the MRSs are achieved with the applied magnetic field through the magnets. Two cases are measured: in case 1, all MRSs are deactivated and in case 2, MRSs 2 and 10 are activated in the unit cells 1 and 3 respectively. The measured results of the reflection coefficient, insertion loss and phase shift are compared with the simulation results. The simulated $|S_{11}| \leq -10$dB and measured $|S_{11}| \leq -8$dB for case 1 in the frequency range (5.38–6) GHz are shown in Fig. 9. The minimum insertion loss $|S_{21}| = -2$ dB and maximum insertion loss is –6 dB for both the cases in Fig. 9.

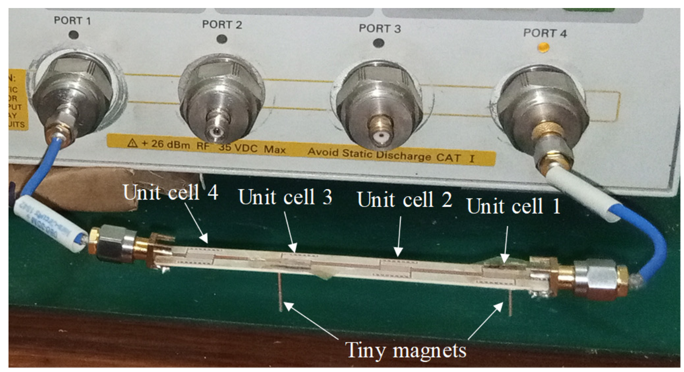

Fig. 8. Measurement setup of fabricated P-CRLH phase shifter connected with network analyzer (model no. E5071C Agilent Keysight).

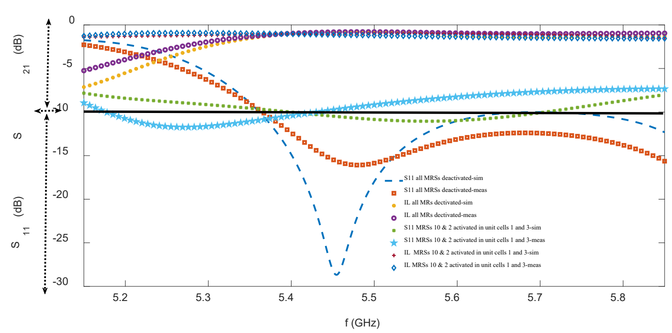

Fig. 9. Comparison of simulation and measured reflection coefficients $|S_{11}|$ and insertion loss $|S_{21}|$ results of the cascaded P-CRLH phase shifter.

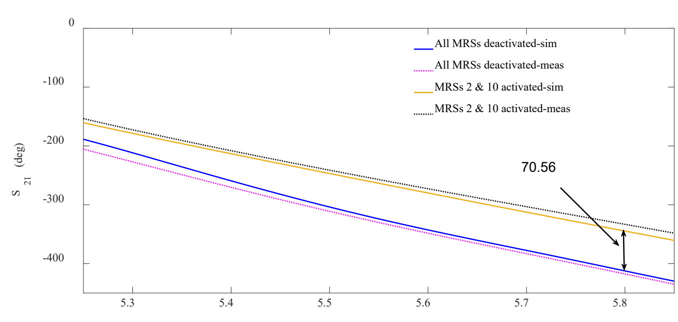

Fig. 10. Comparison of simulation and measured phases $\angle S_{21}$ of cascaded

P-CRLH phase shifter.

The simulated/measured phase response in Fig. 10 shows a 70.56^{o} phase shift between activated and deactivated MRSs. The simulated and measured phase responses are in good agreement within 4 – 5^{o} phase deviation, validating the modeling accuracy discussed in Section II. A similar behavior of the phase response is also demonstrated in [16]-[17].

IV. Singly Curved Conformal Phased Array with Integrated Phase Shifters

For performance analysis, the four unit cell series-connected P-CRLH phase shifters are integrated with 1 × 4 patch antenna array on a curved shaped non-conducting surface bent at30^{o} and 45^{o} angles (θ_B) in CST full-wave simulator as shown in Fig. 11. The spacing between adjacent antenna elements is λ/2 at f_0 = 5.8 GHz. The phase shifts required for main beam at broadside and at 20^{o} scan angle on a singly curved-shaped surface are computed using the projection method in [20] and are given in Table I. The phase shifts obtained with the proposed four unit cell P-CRLH phase shifter are also given in Table I. The required activation of MRSs to achieve phase shifts through the four unit cell P-CRLH phase shifter are numbered in Table II.

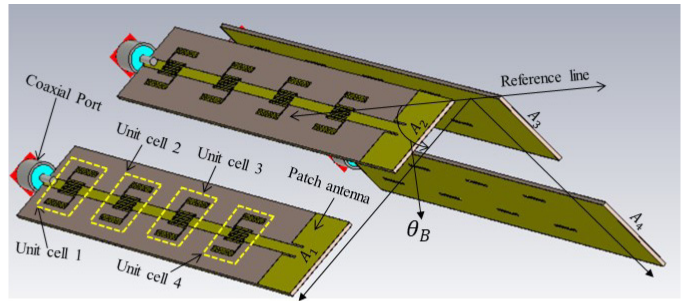

Fig. 11. CST model of the 1 × 4 patch antenna array with integrated P-CRLH phase shifters on the curved surface with bend angle θ_B.

Initially, the 1 × 4 patch antenna array on the curved-shaped surface in Fig. 11 was directly excited (without P-CRLH phase shifters) with the computed phases in Table I. The CST simulated gain patterns for directly excited phases are shown in Fig. 12. Then the same 1 × 4 patch antenna array on the curved-shaped surface in Fig. 11 was excited with the P-CRLH phases in Table 1 and the resulting gain patterns are also shown in Fig. 12. Using the 30^{o} bent curved surface: for broadside pattern, the peak gain is 9.48 dB for directly excited array, and it is 7.38 dB for P-CRLH excited array as shown in Fig. 12(a). For scanned pattern, the peak gain is 9.18 dB for directly excited array, and it is 6.72 dB for P-CRLH excited array as shown in

TABLE I
Computed and simulated phases (degrees) for broadside and 20^{o} main beam scanning (θ_S) on a singly curved-shaped conformal surface with bend angles θ_B = 30^{o} and 45^{o}

Bend angle (θ_B)	Antenna element	Scan angle (θ_S = 0^{o})		Scan angle (θ_S = 20^{o})	
		Computed phases using the projection method [20]	Achieved phases through P-CRLH phase shifter in this work	Computed phases using the projection method [20]	Achieved phases through P-CRLH phase shifter in this work
30^{o}	A_1	-52	-52.43	-87	-87.60
	A_2	-142	-142.21	-115.5	-114.32
	A_3	-142	-142.21	-54	-52.43
	A_4	-52	-52.43	97.5	88.05
45^{o}	A_1	215 or -145	-142.21	-92	-92.34
	A_2	88	88.05	-157.5	-163.24
	A_3	88	88.05	-96	-92.34
	A_4	215 or -145	-142.21	93	88.05

TABLE II
Activated MRSs to achieve the phases in TABLE 1

P-CRLH Phases	MRSs activations in four unit P-CRLH phase shifter (see numbering in Fig. 3)			
	Unit Cell-1	Unit Cell-2	Unit Cell-3	Unit Cell-4
-52.43	OFF	OFF	OFF	0FF
-142.21	1-4,9-12	1-4,9-12	1-4,9-12	1-4,9-12
-87.60	1-6,9-14	1-6,9-14	1-6,9-14	1-6,9-14
-114.32	1-5,9-13	1-5,9-13	1-5,9-13	1-5,9-13
88.05	1,9	1,9	1,9	1,9
-92.34	1-2,9-10	OFF	OFF	OFF
-163.24	1,9	OFF	OFF	1,9

Fig. 12(b). On 45° bent curved surface: for broadside pattern, the peak gain is 8.45 dB for directly excited array, while it is 6.57 dB for P-CRLH excited array as shown in Fig. 12(c). For scanned pattern, the peak gain is 8.15 dB for directly excited array, and it is 6.2 dB for P-CRLH excited array as shown in Fig. 12(d).

The differences in the gains of main beam peak are due to the lack of achieving perfect phases with P-CRLH phase shifter as compared to the computed phases and are also investigated in [17]. Since, the emphasis in this work is on the main beam correction only, therefore, the radiation pattern results of the P-CRLH excited curved conformal array for broadside and scanning case fairly agree with the directly excited array as shown in Fig. 12. The deviations of P-CRLH excited patterns from directly excited patterns (other than peak gain differences) are thought to be due to the mutual coupling effects between P-CRLH phase shifters.

V. Conclusion

A 1 × 4 conformal singly curved-shaped array with integrated magnetically aligned particles inside the composite right/left-handed (CRLH) transmission line working as phase shifter for broadside and main beam scanned at 20° is investigated.

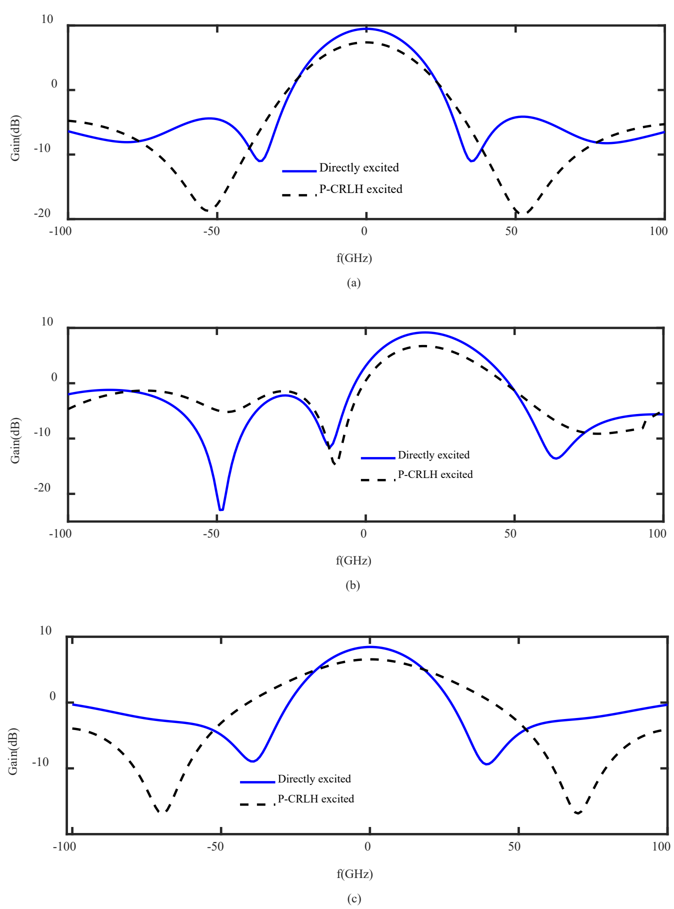

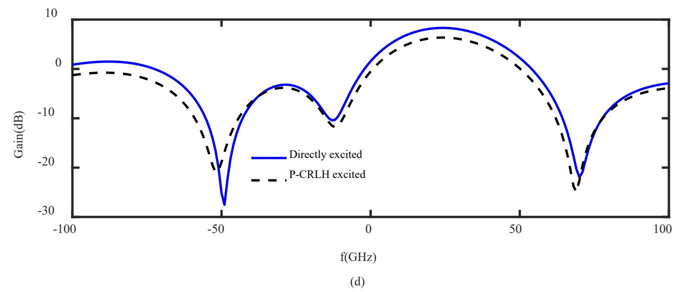

Fig. 12. CST Simulated radiation patterns of a 1 × 4 P-CRLH phase shifters integrated curved-shaped array. (a), (b) are broadside and scanned results on the curved surface with bend angle of $\theta_B = 30°$; and (c), (d) are broadside and scanned results on the curved surface with $\theta_B = 45°$.

The variable phases were obtained as a result of changes in the left-handed (LH) inductance in the proposed CRLH phase shifter. The proposed particles embedded CRLH phase shifter is an alternative solution to conventional diodes based CRLH phase shifter with added advantages of (i) external DC biasing control circuitry is not required, (ii) activation of embedded particles is achieved beneath the ground plane, thus isolating the RF signal from DC biasing circuitry, and (iii) highly suitable for flexible and conformal phased arrays, as there are no discrete components required for its operation. Future work includes investigating the proposed phase shifter on flexible substrates for its uses on fully printable conformal phased arrays.

References

[1] L. Josefsson, and P. Persson, *Conformal Array Antenna Theory and Design*. Wiley-IEEE Press, 2006, ch. 3. DOI: 10.1002/047178012X

[2] Irfanullah, Hina Munsif, and Ali Imram Najam, "Eigenbeam analysis of singly curved conformal antenna array," *Prog. Electromagn. Res. M*, vol. 103, pp. 27–36, June 2021. DOI: 10.2528/PIERM21051204

[3] Irfanullah, B. D. Braaten, A. Iftikhar, S. Nikolaou, and D. E. Anagnastou, "Beamforming with 1 × N Conformal Arrays," *Sensors*, vol. 22, no. 17, pp. 6616, Sept 1, 2022. DOI: 10.3390/s22176616

[4] L. Du, J. Zhao, and J. Xu, "Study on wide-angle scanning characteristics of hemispherical array," *ACES journal*, vol. 37, no. 4, pp. 403–407, Apr. 2022. DOI: 10.13052/2022.ACES.J.370405

[5] T. Bertuch, P. Knott, H. Wilden, and O. Peters, "SAR experiments using a conformal antenna array radar demonstrator," in *Proceedings of the European Conference on Synthetic Aperture Radar (EuSAR'10)*, Aachen, Germany, June 2010.

[6] J-J. Peng, S-W. Qu, M. Xia, and S. Yang, "Conformal phased array antenna for unmanned aerial vehicle with ±70° scanning range," *IEEE Trans. Antennas Propagat.*, vol. 69, no. 8, pp. 4580–4587, Feb. 2021. DOI: 10.1109/TAP.2021.3060125

[7] H. Schippers, et al., "Conformal phased array with beam forming for airborne satellite communication," *2008 International ITG Workshop on Smart Antennas*, Darmstadt, Germany, Feb. 2008. DOI: 10.1109/WSA.2008.4475580

[8] Q. Wang, Z. Su, S. Li, H. Zhao, and X. Yin, "Electrically tunable liquid crystal phase shifter with excellent phase shift capability per wavelength based on opposed coplanar waveguide," *Journal of Physics D: Applied Physics*, vol. 55, no. 40, pp. 405001, July 2022. DOI: 10.1088/1361-6463/ac8127

[9] M. Haghzadeh, H. M. Jaradat, C. Armiento, and A. Akyurtlu, "Design and simulation of fully printable conformal antennas with BST/polymer composite based phase shifters," *Progress In Electromagnetics Research C*, vol. 62, pp. 167–178, Jan. 2016. DOI: 10.2528/PIERC15091504

[10] Z-P. Chen, Z-G Liu, L. Ju, and W-B. Lu, "Beam scanning conformal antenna array with planar integrated phase shifter based on graphene,"

Journal of Materials Science: Materials in Electronics, vol. 33, 14032–14042, May 2022. DOI: 10.1007/s10854-022-08334-2

[11] J. Zhang, S.W. Cheung, and T. I. Yuk, "A compact 6-bit phase shifter with high-power capacity based on composite right/left-handed transmission line," *The 40th European Microwave Conference*, Paris, France, Sept. 2010. DOI: 10.23919/EUMC.2010.5616000

[12] S-H Hwang, T. Jang, J-M. Kim, Y-K. Kim, S. Lim, and C-W. Baek, "MEMS-tunable composite right/left-handed (CRLH) transmission line and its application to a phase shifter," *Journal of Micromechanics and Microengineering*, vol. 21, pp. 1–12, Nov. 2011. DOI: 10.1088/0960-1317/21/12/125022

[13] Y. S. Wu, X. Q. Lin, J. Zhang, Y. Jiang, F. Cheng, and Y. Fan, "Broadband and wide range tunable phase shifter based on composite right/left handed transmission line," *Journal of Electromagnetic Waves and Applications*, vol. 26, no. 10, 1308–1314, July 2012. DOI: 10.1080/09205071.2012.699386

[14] A. Iftikhar, J. Parrow, S. Asif, J. Allen, M. Allen, and D.B Braaten, "Improving the efficiency of a reconfigurable microstrip patch using magneto-static field responsive structures," *Electronics Letters*, vol. 52, pp. 1194–1196, July 2016. DOI: 10.1049/el.2016.0827

[15] Potters Industries LLC. Available online: http://www.pottersbeads.com/ (accessed on 16 May 2023).

[16] M. Ayaz, A. Iftikhar, B. D. Braaten, W. Khalil, and I. Ullah, "A composite right/left-handed phase shifter-based cylindrical phased array with reinforced particles responsive to magneto-static fields," *Electronics*, vol. 12, no. 2, pp. 306, Jan. 2023. DOI: 10.3390/electronics12020306

[17] M. Ayaz, and I. Ullah, "A phased array antenna with novel composite right/left-handed (CRLH) phase shifters for Wi-Fi 6 communication systems," *Appl. Sci*., vol. 13, no. 4, pp. 2085, Feb. 2023. DOI: 10.3390/app13042085

[18] A. Lai, T. Itoh, and C. Caloz, "Composite right/left-handed transmission line metamaterials," *IEEE Microwave Magazine*, vol. 5, no. 3, pp.34–50, Sept. 2004. DOI: 10.1109/MMW.2004.1337766

[19] J. Parrow, "Equivalent circuit modeling and signal integrity analysis of magneto-static responsive structures, and their applications in changing the effective permittivity of microstrip transmission lines," Ph.D. dissertation, Dept. Elect. Eng., North Dakota State University, Fargo, 2016. https://library.ndsu.edu/ir/handle/10365/28002

[20] B. D. Braaten, S. Roy, S. Nariyal, M. A. Aziz, N. F. Chamberlain, Irfanullah, M. T. Reich, and D. E. Anagnostou, "A self-adapting flexible (SELFLEX) antenna array for changing conformal surface applications,", *IEEE Trans. Antennas Propagat*., vol. 61, no. 2, pp. 655–665, Feb. 2013. DOI: 10.1109/TAP.2012.2226227